Journal of Tribology Science and Technology
Original Research Article
Publication Date: 14 August 2024
Submission Date: 04 May 2024
DOI: 10.70973/JTST.1.1.2024.1-14

ROLE OF POLYSACCHARIDES-BASED GREEN FILLER ON MECHANICAL PROPERTIES AND SCRATCH RESISTANCE OF EPOXY COMPOSITES

Jaswant K Hirwani*, Shanmukhi Sripada and Sujeet K Sinha

Department of Mechanical Engineering
Indian Institute of Technology Delhi, Hauz Khas, New Delhi 110016, India
*Corresponding author (e-mail: jaswant.hirwani@gmail.com)

ABSTRACT

Gum acacia (GA) reinforced epoxy composites were characterized for their mechanical and structural properties. In compression test, increasing trend of modulus and decreasing trend of strength and toughness led to the optimized composition of 10 wt.% of GA in epoxy (GA-10). Increased modulus could be due to the intermolecular bonding through polar group interaction between SU-8 and GA molecules. This interaction was confirmed by –OH peak reduction in FTIR analysis. Modulus increase could also be due to the presence of rigid GA particles, but the decrease in strength and toughness was attributed to the presence of voids and high-stress concentration points around GA particles. Vickers hardness increased by 17.8% for GA-10 compared to pure SU-8. Both scratch width and depth were lower for GA-10 than SU-8 except at 400 g load. These results project GA as a choice of filler to improve mechanical properties and scratch resistance of polymers.

KEYWORDS: Polysaccharides; gum acacia; SU-8; scratch; wear

1. INTRODUCTION

In the past decade, many natural or bio-based fillers have been utilized to fabricate epoxy-based composites for structural applications. This shift towards natural fillers is due to their eco-friendly nature compared to synthetic fillers. Most of the synthetic fillers are either metallic or derived from petroleum-based sources. Processing with metals is health hazardous to workers, not only during the manufacturing stage but also at the recycling stage. Petroleum-based fillers are generally toxic and non-renewable, and hence, their utility should be minimized.

In contrast, nature-based fillers are non-toxic, biodegradable, easily disposable, and possess low energy production costs. Therefore, many researchers have directed their work towards nature-based fillers obtained from plant sources. It is well understood that the properties of these plant-based extracts may vary depending upon the source location. They may not fully replace the synthetic fillers, but exploring them for possible applications can lead to a sustainable technology in the future.

Natural cellulosic fibers have been the most exploited plant-based products due to their low density and higher strength-to-weight ratio (Abdul Khalil, *et. al.*, 2012; Onuaguluchi and Banthia, 2016; Li *et al.*, 2020; Zhang *et al.*, 2020). For example, Lignocellulosic fibers (*consists of both carbohydrate and lignin polymers*) such as kenaf, jute, hemp, sisal, ramie, banana, and pineapple leaf have been explored for different applications such as wood-plastic composites, lightweight building materials, and door panels, etc. (Basta, *et. al.*, 2004; Reddy and Yang, 2005; Satyanarayana, *et.al*, 2007; Ashori, 2008; Satyanarayana, *et.al.*, 2009; Ibrahim *et al.*, 2010; Monteiro *et al.*, 2011; Das, 2017; Yang, Ching and Chuah, 2019; Youssef *et al.*, 2019). Another essential plant-based carbohydrate polymer is exudate gum, which is a polysaccharide-protein complex and has been used for many household and industrial applications (Verbeken, *et.al.*, 2003; Williams and Phillips, 2009). It is a gummy discharge of plants produced as a natural defense mechanism to seal bark wounds. One of the primarily used exudate gum is gum acacia.

Historically, its usage can be dated back to around 5000 years ago as a mineral paint adhesive for making hieroglyphs (Whistler and BeMiller, 2012). It has excellent emulsifying, stabilizing, thickening, and binding characteristics, and hence it is a popular natural ingredient in ice creams, jellies, candies, soft drinks, syrups, and chewing gums (Dickinson *et al.*, 1988; Dickinson *et.al*, 1989; Grein *et al.*, 2013; Singh, *et.al.*, 2017; Adam Mariod, 2018). It is also used as a coating and glaze product in confectionery items due to its film-forming ability. Binding property makes them suitable in conventional art applications such as water-based color painting, lithography, and printing (Chudzikowski, 1971; Whistler and BeMiller, 2012; Ferreira *et al.*, 2019). The adhesive behavior makes them suitable for blushers and similar cosmetic products (Verbeken *et.al.*, 2003). Carboxylic acid (-COOH) and hydroxyl group (-OH) are the major functional groups in GA, available for functionalization and cross-linking with other polymers (Daoub *et al.*, 2018). It can be used for increasing the mechanical strength of polymers or polymer composites because of its good binding and adhesive properties. Recently, few research groups have proved its potential as a polymer composite filler material. A hydroxyapatite/gum acacia nanocomposite was prepared for drug delivery and tissue engineering application (Padmanabhan *et.al.*, 2018). An edible gum acacia/chitin composite coating was prepared to control postharvest anthracnose of banana during cold storage (Maqbool *et al.*, 2010). An epoxy/gum arabic composite was suggested as an anticorrosive and self-healing coating for steel substrates under marine conditions (Arukalam *et al.*, 2020). It is clear from the current literature that its functional properties have been utilized to obtain the end product's desired functionality. However, there are lack of experimental evidences on how these properties can affect the mechanical performances of a composite. In our previous work on polymer composites with GA filler, some promising results were obtained in this direction (Hirwani and Sinha, 2021). Hence, in this paper, we tried to explore detailed mechanical characterization of GA-filled composite, and few correlations have been established with its structural properties.

Previously, many fillers have been utilized to improve the mechanical and tribological properties of epoxies (Low *et al.*, 2007; Sinha *et al.*, 2009; Nirmal *et.al.*, 2012; Barari *et al.*, 2016; Sarkar *et.al.*, 2018; Huang and Young 2019; Megahed *et al.*, 2019). They majorly focused on fiber-type fillers from natural sources but not particulate fillers. Fiber fillers perform better when loading is majorly tensile or bending type but not in compression, as buckling limits their performance. Another category is particulate-filled composites that can perform better in compression, and if it is coupled with adhesive properties, it can be well suited for tensile conditions. GA is such a bio-based particulate filler that has not been explored much. We hypothesize that polar groups of both epoxy and GA can have some chemical interaction. These interactions can play a significant role in improving the composite's mechanical, scratch, and thermal properties. So, in this paper, an effort has been made in this direction. Commercially available epoxy (SU-8) consisting of eight epoxy groups in a single molecule was selected as the matrix. The structures of SU-8 and a polysaccharide side chain of GA are shown in Fig. 1. SU-8 and its composites have been already used for microelectromechanical systems and bio-applications (Saravanan *et.al.*, 2013; Hirwani and Sinha 2021; Arshad *et. al.*, 2020).

2. EXPERIMENTAL METHODS

2.1. Materials and sample preparation

SU-8 epoxy (monomer viscosity of 4500 cSt and density 1.219 g/ml) was purchased from MicroChem Corp USA. Triethylenetetramine-based curing agent with the trade name Aradur HY 951 was supplied by Huntsman International India Pvt. Ltd. (viscosity 15 mPa-s and density 0.98 g/ml). GA powder which had an aspect ratio of 0.69 ± 0.17, was used in this study. Before composite fabrication, SU-8 filled in a beaker was heated on a hot plate at 40^{o}C for 2-3 minutes to reduce the viscosity. GA powder was added in a fixed ratio to SU-8 liquid and stirred properly to obtain a homogeneous solution. Finally, the curing agent was added to start cross-linking process. The mix was placed in a transparent plastic bag, and the bubbles were physically removed by mechanically pushing out from the bulk of mix. After the oven curing process, all the samples were kept for 18 days at room temperature to ensure completion of the cross-linking, as the specimen showed a continuous increase in mechanical properties by slow curing reaction. For compression and hardness test, cylindrical samples, for tensile test, dog-bone samples, and for scratch test, rectangular strip type samples were prepared.

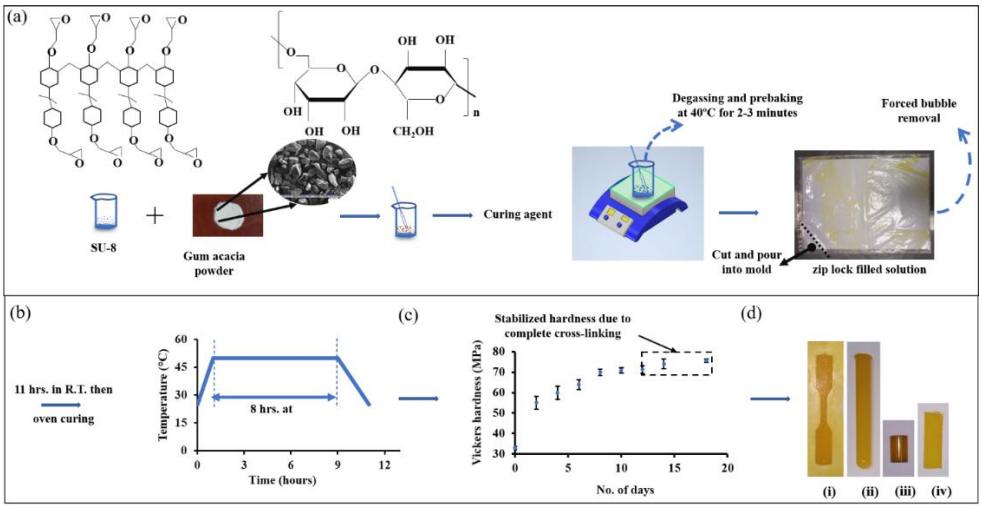

Fig. 1. (a) Fabrication process of SU-8/GA composites, (b) curing process in oven, (c) room curing and hardness stabilization, and (d) cured samples for (i) tensile (ii) compression, (iii) hardness, and (iv) scratch tests

Fig. 1 shows all the steps of sample fabrication adopted in this study and images of all the samples fabricated for testing. Four different samples were prepared with different wt.% of GA, including pure SU-8 sample. They are designated as SU-8, GA-5 (SU-8 with 5 wt.% GA), GA-10 (SU-8 with 10 wt.% GA), and GA-15 (SU-8 with 15 wt.% GA).

2.2. Bulk mechanical properties and scratch resistance

Compression and tensile testing of the composites were performed according to the ASTM D 695 and ASTM D 638, using Shimadzu Universal Testing Machine at cross-head speeds of 1.3 and 1 mm/min, respectively, at ambient temperature. Vickers hardness was measured on a flat surface using hardness tester supplied by Invogineeirg Pvt. Ltd. A square base pyramidal diamond indenter with an apex angle of 136° was used with a normal load of 840 g and a dwell period of 12 s. The following equation was used for hardness measurement.

$$HV = \frac{1.854\ F}{d^2}$$

Where *HV* represents Vickers hardness in MPa, *F* indicates load in N, and *d* is the mean diagonal length of indent (mm). Scratch test was conducted at four different constant loads of 200, 300, 400, and 500 g for each of the pure SU-8 and composite samples. The scratch length and speed were selected as 15 mm and 2 mm/s, respectively. A 60° high speed steel (HSS) conical indenter was used for the test.

2.3. Characterization of composites

To obtain the molecular and microstructural information of the composites and correlate them with the mechanical performances, Fourier-transform Infrared Spectroscopy (FTIR) and X-Ray Diffraction (XRD) were conducted on powdered samples. For FTIR, Nicolet FTIR spectrometer was used in attenuated total reflection mode. The spectrum region was 450 to 4000 cm^{-1}. XRD (RIGAKU ULTIMA-IV) with CuKα, X-ray radiation (λ = 0.154178 nm) was conducted at a scan speed of 4°/minute. 3-D optical profilometer and scanning electron microscope (SEM) were used to analyze the surface characteristics of the composites. Thermo-gravimetric analysis (TGA) was conducted using TA Instruments, SDT Q600 in the range of 50 to 800 °C at 20 °C/min heating rate in a nitrogen atmosphere.

3. RESULTS AND DISCUSSION

3.1. Curing process optimization

We observed the significant change in the hardness of oven cured samples during post-cured self-aging at room temperature. This was due to the increase in cross-link density during the storage. Therefore, to obtain a fully stabilized sample, the oven-cured samples were kept for 18 days at room temperature in a desiccator before any test was performed. The hardness value measured at an interval of two days is shown in Fig. 1 (c). Data obtained for 14th and 18th days are close to each other as the room temperature curing had saturated after this period. All the samples of SU-8 and GA-filled composites were prepared by this method.

3.2. Cross-section analysis

Fig.2 shows SEM images of cross-section of composites which was brittle fractured in liquid nitrogen.

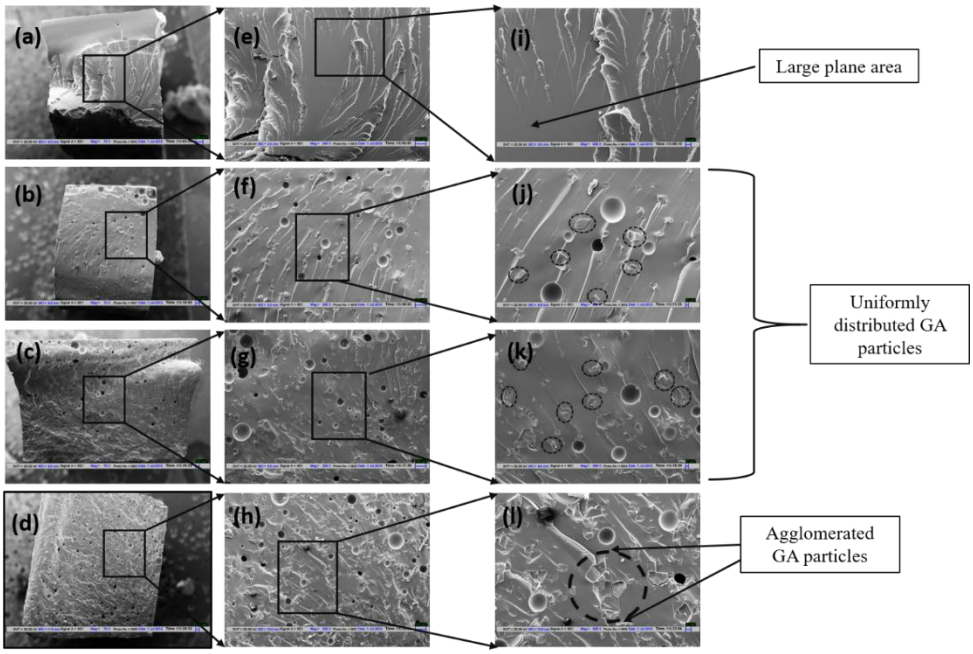

Fig. 2. SEM images of brittle fractured cross-section of (a) SU-8 (b) GA-5 (c) GA-10 (d) GA-15 composites and corresponding magnified images showing the distribution of GA particles.

It can be seen, SU-8 sample is clear in the absence of filler material, and no void formation was observed (Fig. 2a, e, i). As we increase the wt. % of GA, the void formation also increased (Fig. 2a, b, c, d). This can be attributed to the increased viscosity of higher wt.% of GA composite before pouring. It was difficult to prepare samples with higher wt.% of GA due to the increased viscosity. Hence, we could only make up to 15 wt.% composite. In all the composites (see Fig. 2j, k, l), particles are marked with a black circular region which depicts well-distributed filler material. In the GA-15 sample, some sites were found to have an agglomeration of GA. This could be attributed to the higher viscosity of GA-15 solution, which hindered the mobility of filler particles.

3.3. Mechanical test

3.3.1. Compression and tensile test

Our objective was to improve the overall mechanical properties and scratch resistance of SU-8 epoxy by GA filler addition. With this aim, we first performed a compression test. We have optimized the elastic modulus, strength, and toughness of the composite obtained from the compression test. The stress-strain curve is shown in Fig. 3a. Elastic modulus, ultimate compressive strength, and toughness of the composites were calculated from the stress-strain curves and are presented in Fig. 3 b, c, and d. An increment in the elastic modulus was observed with the increasing percentage of the filler addition, which is in good agreement with the results published for different epoxy composites (Radford, 1971; Spanoudakis and Young, 1984). GA-15 has the highest modulus of 1065 MPa compared to 784 MPa for the pure SU-8 sample. An increase in modulus can be attributed to the stiff and rigid filler of gum powder, while the decrease in strength and toughness of the composite could be due to early crack propagation inside the matrix. The GA particles had an irregular shape and pointed edges which would have caused higher stress concentration points throughout the matrix. The failure strain of the composites decreases with an increase in filler concentration, which justifies the generation of high-stress concentration points around the GA particles. It has also been observed that GA-filled composite contains voids (Fig. 2) which again weakens the overall strength of the composite. Since the strength and toughness also depend upon the matrix–filler bonding, there is an opportunity to further improve the mechanical properties by surface modification of filler particles. For example, silane functionalized Graphene oxide shows an increased strength and fracture toughness of the epoxy composite (Wan *et. al.*, 2014). This way, we can eliminate the negative effect of the particle shape and voids in the composite and thus avoid the generation of localized stress points, which resulted in early failure. All the quantitative data from Fig. 3 are provided in Table 1. Yield strength of the composite is also an important criterion for material selection. The yield strength measured was 24, 31.30, 33.04, and 32.67 MPa for SU-8, GA-5, GA-10, and GA-15, respectively (measured by the 0.2% offset strain method). It shows that GA-10 has the highest value obtained from these composites. Further, the increasing trend of modulus and decreasing trend of the strength and toughness leads to the optimized composite of 10 wt.% GA filler, i.e., GA-10. Hence, we chose GA-10 as the optimized composite for further analysis and to understand the effects of GA on other mechanical, structural, and thermal properties. It should be noted that for GA-10, the modulus was increased by 29.8 %, and ultimate strength and toughness

decreased by 30.3 and 22.4%, respectively, compared to pure SU-8.

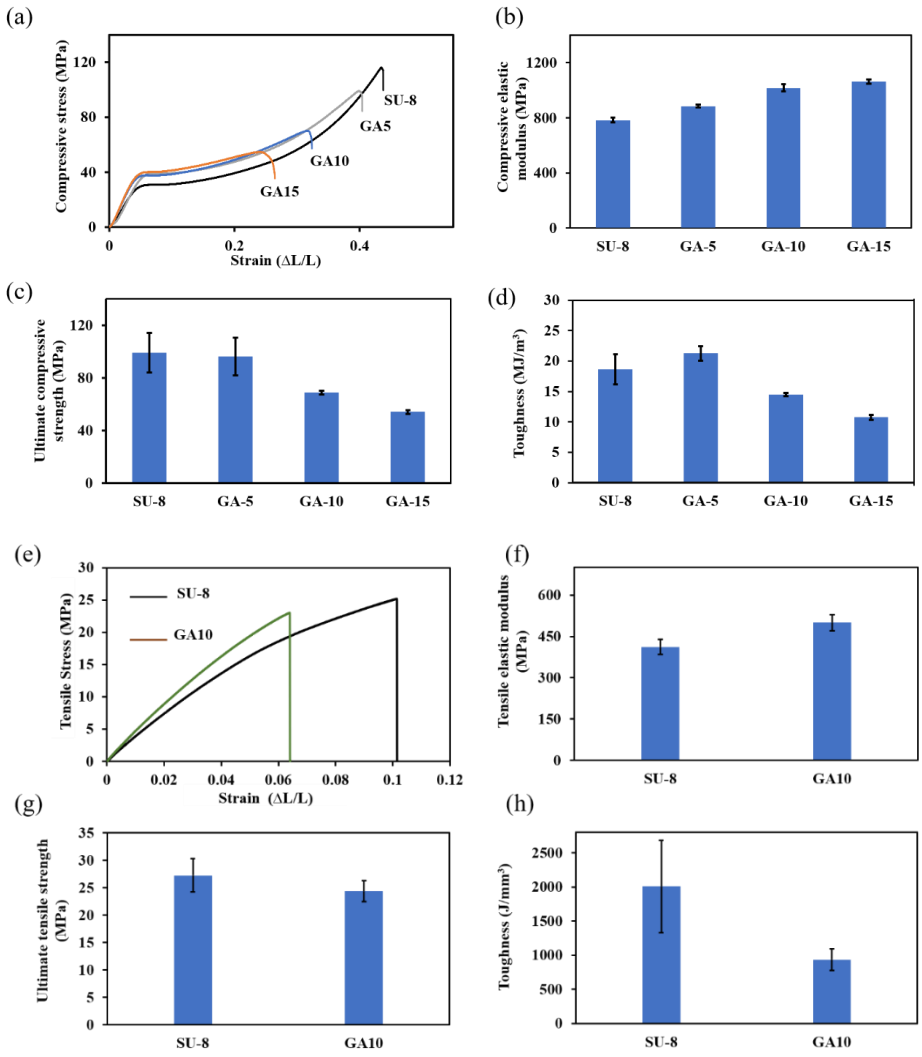

Fig. 3. Represents stress-strain curve with their mechanical properties, (a) to (d) represents compression and (e) to (h) represents tensile test.

Table 1. Compression (C) and tensile (T) test data for all the SU-8 composites

Composites	Elastic Modulus (MPa)	Ultimate strength (MPa)	Toughness (MJ/m^3)	Elongation at break (%)
SU8 (C)	784 ± 19	99 ± 15.00	18.64 ± 2.50	41.50 ± 2.95
GA 5 (C)	885 ± 9	96 ±14.00	21.22 ± 1.23	40.30 ± 1.90
GA 10 (C)	1018 ± 24	69 ± 1.60	14.47 ± 0.25	31.23 ± 1.08
GA 15 (C)	1065 ± 16	54 ± 1.32	10.72 ± 0.37	24.30 ± 0.00
SU-8 (T)	412 ± 27	27 ± 3.01	2007 ± 678	0.11 ± 0.015
GA-10 (T)	500 ± 30	24 ± 1.90	934 ± 157	0.06 ± 0.003

The tensile stress-strain curve is plotted in Fig. 3 e, and other properties are shown in Fig. 3 f, g, and h. The numerical values are presented in Table 1. Both SU-8 and GA-10 composite shows a brittle fracture in tension, as the absence of yielding phenomena depicts the same. The absence of yielding is due to the composite's premature failure. In tensile test, cracks and void opens up during stretching while during compression they close and promote a chance of yielding before fracture. With the GA addition, elastic modulus increased by 21.4 %, but the ultimate strength and toughness were decreased by 11.1 and 53.5 %, respectively.

SEM images of tensile fractured samples are shown in Fig. 4. For SU-8, fractography images show a river-like structure, typical for brittle materials (Khan *et.al.*, 2017). We can divide crack propagation into three different zones. The first is crack initiation, the second is crack growth, and the third is mature crack propagation and ultimate failure. Initially, the crack started growing up by changing the propagation direction by the crack shift angle of 133º. In the second and third regions, the crack length is larger, separated by wider plane areas. Few localized failure points were also observed, indicative of plastic deformation (Fig. 4 a.1).

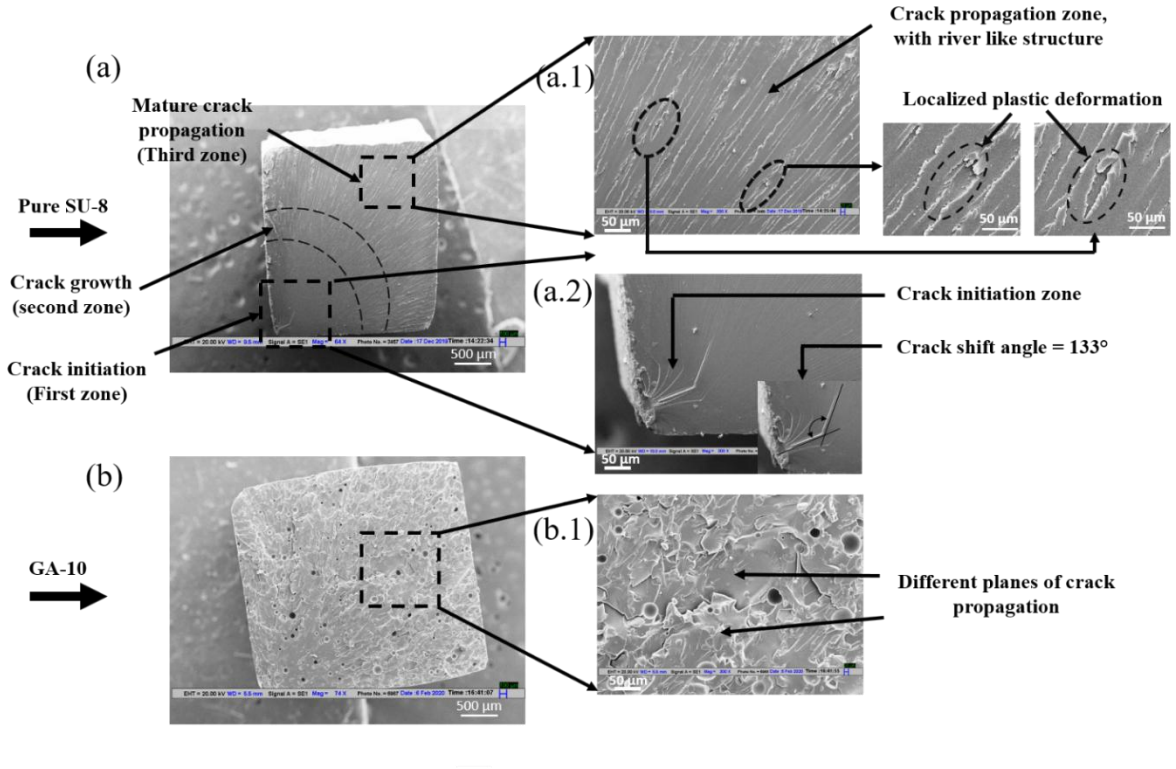

Fig. 4. Tensile fractography images were observed by SEM for (a) SU-8 and (b) GA-10 composite.

It is generally accepted that multiple fracture points indicate more energy absorption for breaking, which leads to tougher material, but GA-10 composite shows the reduction in ultimate fracture stress, resulting in lower toughness. This could be due to the presence of different localized stress boosters (voids and sharp edges around gum particles), leading to the generation of different crack planes (Fig. 4 b.1). Hence, it would result in lower strain required for failure, and also the toughness was less in comparison to SU-8.

3.3.3. Micro-hardness vs. yield strength

In Fig. 5 a, we can see GA-10 sample has a higher hardness value of 86 MPa compared to 73 MPa for SU-8. These results confirmed the stiff and rigid nature of GA particles, resulting in higher elastic modulus.

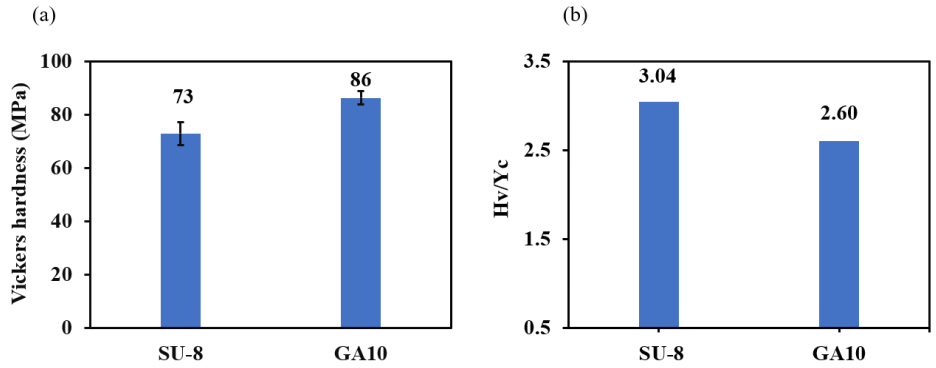

Fig. 5. (a) Micro-hardness and (b) H_V/Y_C ratio of the SU-8 and GA-10 composites

To categorize the material as elastic, plastic, or elastoplastic, both hardness and yield strength are needed. We also calculated the ratios of Vickers hardness to compressive yield strength (H_V/Y_C) for both samples. To calculate H_V/Y_C, average hardness value and average yield strength data were taken, and hence no standard deviation has been shown in the presented graph. From the well-known Tabor's relation $H \approx 3Y$ (Tabor D, 1970), we can predict the nature of the samples. Flores *et. al* (Flores *et al.*, 2000) has discussed the micro-hardness correlation with the yield strength for chain extended polyethylene and concluded that hardness is nearly three times the tensile yield strength ($H_V \sim 3Y_t$), but during compression, this relationship changes to $H_V \sim 2Y_C$. This could be due to higher compressive yield strength compared to tensile one. We observed that SU-8 sample has a H_V/Y_C value around 3.04 which indicates the plastic nature of the sample. GA-10 sample has a value of 2.61 indicating the presence of stiffer filler material, gum acacia. We also expect some reduction in hardness value due to the presence of voids. Both these factors could have contributed to lower *H/Y* ratio. Based on the values of *H/Y* factor we can consider GA-10 to be more brittle than SU-8.

3.4. Scratch test

Scratch test is used for quick and easy analysis of materials response against abrasion by hard surfaces. Fig. 6 (a) and (b) shows the scratch surfaces of SU-8 and GA-10 composite, respectively. Width of scratch was measured at the middle of the track at three different locations, and average values were plotted for representation. Accurate depth measurement was quite difficult, due to larger deviation in the data. Therefore, we choose highest value of the three measurements for comparison. With the increase of load from 200 to 500 g width, and depth of scratch increased for both SU-8 and GA-10 samples.

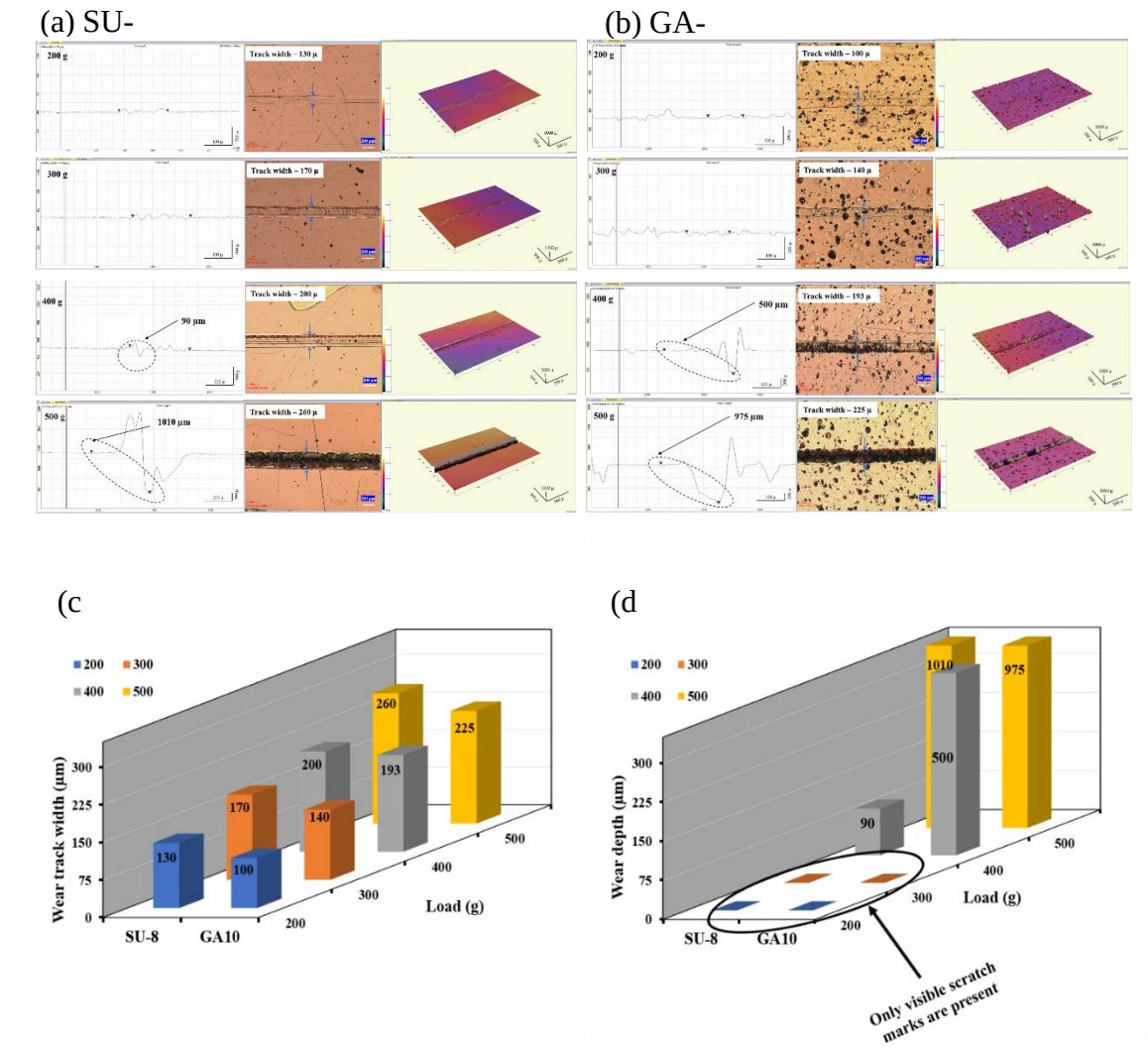

Fig. 6 (a) and (b) shows 3D Optical profilometery after scratch test; (c) and (d) represents scratch track width and depth of, respectively.

For SU-8 sample, width of the scratch increased from 130 to 260 µm and depth increased from negligible value (plastic deformation) to 1010 µm (severe wear). Similarly, for GA-10 composite, scratch width increased from 100 to 225 µm, and the depth values reached 975 µm (severe wear) from negligible value (elastic deformation) at 200 g. This increase in width and depth with load could be due to higher penetration of indenter tip during the progression of scratch. In the case of SU-8, if the load is below 300 g, we could only observe the change in surface profile after scratch. No removal of material can be seen, and a visible scratch indicates minor plastic deformation. The same conclusion can be drawn from GA-10 samples, but the visibility of scratch is poorer compared to SU-8, which is an indication of more elastic than plastic deformation. This could be due to higher bulk mechanical properties (elastic modulus, yield strength, and hardness) of GA-10 composite, which promotes less plastic deformation for the same scratch load. At the normal load of 400 g, the GA-10 sample has a higher scratch depth (500 µm) compared to SU-8 (90 µm), which could be due to the removal of some GA particles as well as exposed voids present on GA-10 composite. Again, at 500 g, both SU-8 and GA-10 samples show severe wear, causing more wear debris. But for GA-10, the scratch track width and depth are less (i.e., 225 and 975 µm, respectively) due to higher hardness compared to SU-8. Track width and scratch values are presented in Fig. 6 (c) and (d).

SEM images after the scratch test are shown in Fig. 7. At 200 g load, scratch visibly is poor for SU-8 and GA-10 samples. At 300 and 400 g load, a periodic parabolic zone can be seen with the vertex of the parabola pointing opposite to the direction of the scratch. These cracks are typical for brittle polymer and have been previously reported for epoxy and glass materials (Lawn *et.al.*, 1984; Jiang *et.al.*, 2009). Another author has reported these features for PMMA as excessive brittle cracking with an arrowhead pointing opposite to scratch direction

(Briscoe *et.al.*, 1996). At 400 g normal load, the GA-10 sample shows the presence of some micron-sized cracks and holes, which indicate the presence of voids on the samples. This could be one of the reasons for the higher depth in the case of GA-10. For brittle polymer, it is known that increase in rigidity (modulus) causes stress concentration which leads to the generation of cracks during scratching. Higher surface roughness of GA-10 (R_a = 2.4) compared to SU-8 (R_a = 0.92) could also have contributed to higher friction and higher tensile stress at the rear side of the tip (Briscoe and Sinha, 2003). This high value of tensile stress contributed to crack formation in GA-10. At 500 g load, higher penetration depth causes higher friction values, and hence stick-slip phenomenon was observed for both samples. For the GA-10 sample, the "stick" period is longer (1970 µm) compared to that for the SU-8 sample (1110 µm). This could be due to solid GA particles, which created an obstacle for tip movement and increased the friction during scratch.

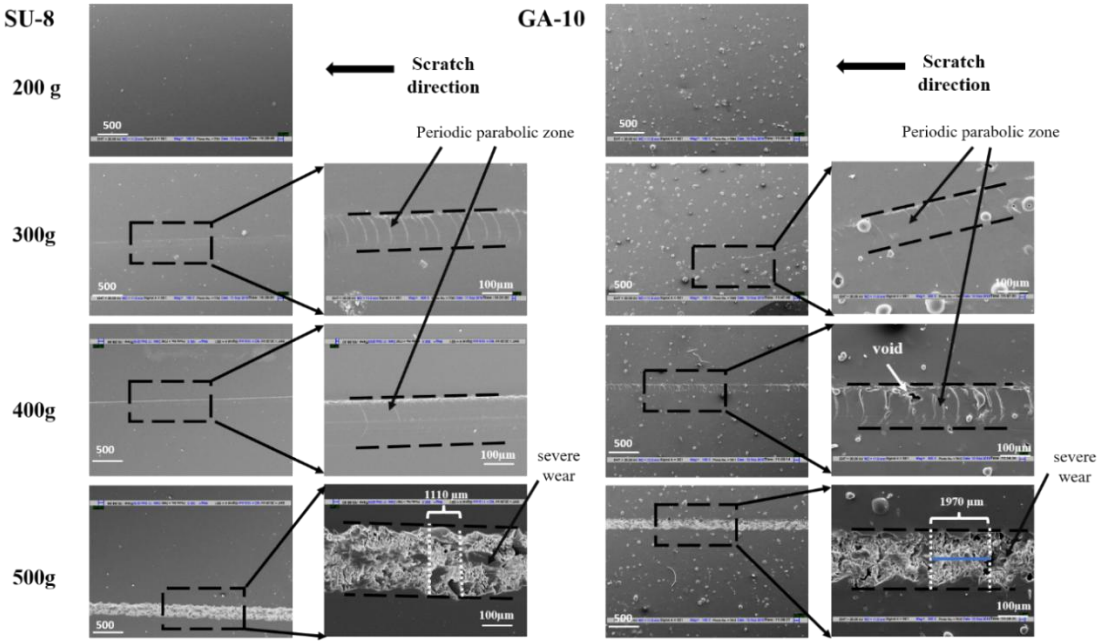

Fig. 7. SEM micrograph of SU-8 and GA-10 samples after scratch testing at different loading conditions.

3.5. Micro-structural analysis

3.5.1. FTIR and XRD analysis and proposed mechanism

To understand the chemical interaction between the SU-8 matrix and GA particles, FTIR analysis was conducted. Fig. 8 (a) shows the individual IR spectrum for SU-8, gum particles, and GA-10 composites. Table 2 shows significant peak intensities present on all the samples. Hydrophilic SU-8 should contain both hydroxyl (from uncured SU-8) and amine groups (from amine-based hardener). The presence of a broad –OH peak at 3480 cm^{-1} could have hindered amine peaks, which is usually found as sharp doublet around 3300-3500 cm-1. Another significant change is the reduced intensity of –OH peaks for GA-10 composite (at 3391 cm-1) compared to gum powder sample (at 3286 cm-1). This could be due to the consumption of the hydroxyl group in reaction with SU-8. The byproduct water evaporated during oven curing. The reaction mechanism has been shown in Fig. 8 (b).

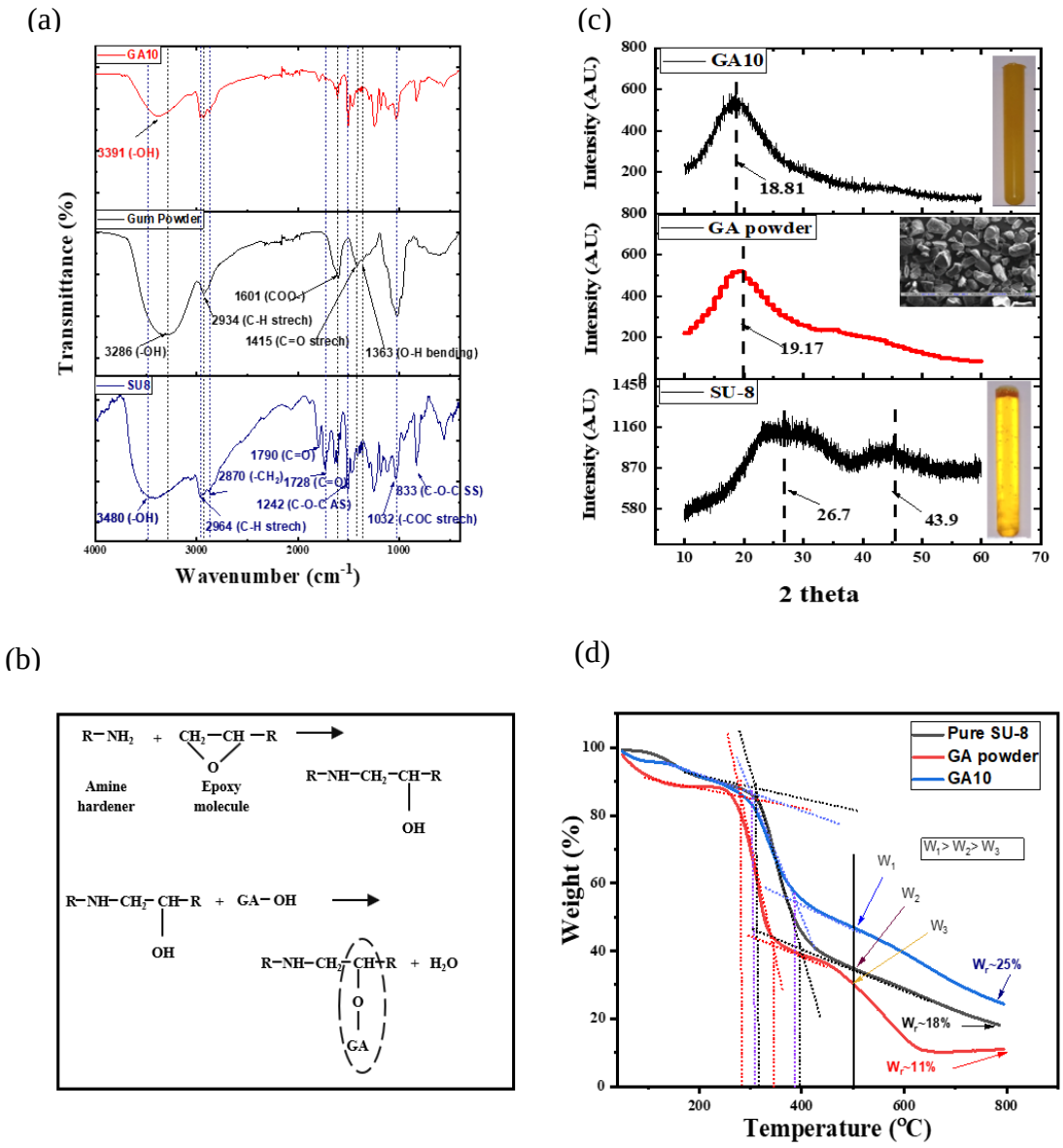

Fig. 8. (a) and (b) show the FTIR analysis and proposed reaction mechanism between SU-8 and GA powder in the presence of amine-based curing agent (c) and (d) XRD and TGA analysis of SU-8, GA powder, and GA-10

Table 2. All the FTIR peak intensities of SU-8, GA powder, and GA-10 composites

Wavenumbers (cm^{-1})	SU-8	GA powder	GA-10 composite
3286		-OH	
3391			-OH
3480	-OH		
2964	-CH Stretch		-CH Stretch
2934		-CH Stretch	
2870	$-CH_2$ Stretch		$-CH_2$ Stretch
1790	-C=O		-C=O
1728	-C=O		
1601		$-COO^-$	$-COO^-$
1542	-C-O-C (AS)		-C-O-C AS
1415		-C=O Stretch	
1363		-OH Bending	
1032	-COC Stretch		-COC Stretch
833	-C-O-C (SS)		-C-O-C (SS)

*AS – Asymmetric stretch

**SS – Symmetric stretch

The shift in the peak intensity is also an indication of chemical interaction between the two groups. All the other peak intensities of GA-10 are primarily due to both the compounds in a single solid.

In XRD analysis (Fig. 8 c), two broad peaks at 2θ =26.7º and 43.9º show the amorphous nature of SU-8. GA powder also indicates an amorphous nature, but the hump is less broad than SU-8. A similar characteristic was observed for the GA-10 composite at 2θ =18.81º. Therefore, we can conclude that all three samples show amorphous behavior with slight increase in crystallinity for the GA-10 composite. A shift in diffraction peak from 26.7º to 18.81º also indicates the interaction between the filler and the matrix.

3.5.2 TGA analysis

Fig. 8 (d) shows the TGA curve for all the samples. For SU-8, the initial reduction in weight is due to adhered and bound water and unreacted solvent of SU-8. After that, second stage degradation starts at 315ºC which ends at 399ºC. This corresponds to the degradation of SU-8 molecules. GA powder also shows the characteristics of moisture loss up to 180ºC. Among all the samples tested, the curve's initial slope is highest for the GA sample, which indicates the presence of a large amount of adsorbed water molecules. This result is in line with the FTIR data (Fig. 8 (a)). Loss of polysaccharides molecule is the second stage degradation which ends at 630ºC. Since initial degradation of GA starts earlier (272ºC) than the SU-8 molecule (315ºC), GA-10 composite initial degradation temperature is lower than that of the SU-8. This could be due to the initiation of degradation of polysaccharides. Although degradation starts at an early stage, the composite is more stable compared to SU-8. This can be attributed to the intumescent effect (coating of char component on SU-8

polymer produced during heating of GA). A similar mechanism has been presented elsewhere (Basak and Ali, 2017). A vertical line drawn at a temperature of 500ºC indicates more residual weight for GA-10 than SU-8 ($W_1>W_2>W_3$). At the end of the experiment, the same sequence was followed with a higher char yield of 25% for GA-10 composite compared to 18% for SU-8. These evidences show that GA increases the thermal stability of SU-8. SU-8 and GA can interact with each other through condensation reaction, producing water molecules (the mechanism is shown Fig. 8 (b)). Such interaction between two polymers can lead to intermolecular cross-links, thereby restricting their movements within the matrix. This could also be one of the reasons for higher elastic modulus for GA-10 composite both in tensile and compression test.

CONCLUSIONS

Effects of GA filler (which is *a plant-based particulate polysaccharide*) on the mechanical properties and scratch resistance of epoxy composites were studied. Filler composition was optimized based on the mechanical test. To understand the molecular, microstructural, and thermal characteristics of the optimized composite, FTIR, XRD, and TGA analysis were carried out. Based on these experiments following conclusions can be drawn.

1. GA-10 composite containing 10 wt.% of GA was the optimized composite, showing increase in compression and tensile moduli by 29.8 and 21.4%, respectively. Ultimate strength and toughness were decreased by 30.3 and 22.4% for compression and 11.1 and 53.5% for tensile tests, respectively, over SU-8.
2. GA-10 composite has shown Vickers hardness increase by 17.8% compared to SU-8. Higher stiffness of the gum acacia filler particles improved the abrasion resistance of the composite, which has been confirmed from the scratch width and depth profiles.
3. The matrix-filler interaction has been confirmed by FTIR analysis, where a significant peak shift from 3480 cm^{-1} to 3391 cm^{-1} and reduction in peak intensity was observed. The underlying reaction mechanism is also proposed, which justifies the decrease in hydroxyl peak.
4. XRD analysis has also confirmed the chemical interaction between the matrix and filler material by the shift in diffraction angle.
5. The intumescent effect could have contributed to an increase in the thermal stability of the composite.

Overall, it is concluded that GA can be utilized to improve the mechanical properties and scratch resistance of epoxy composites. It is also noticed that further modification in composite preparation would be required to improve the strength and toughness of the composite.

CRediT authorship contribution statement

Jaswant K Hirwani: Conceptualization, Methodology, Validation, Formal analysis, Visualization, Writing - original draft. Shanmukhi Sripada: Investigation, Methodology, Visualization, Formal analysis, Data curation, Sujeet K Sinha: Conceptualization, Methodology, Validation, Visualization, Writing - review and editing, Supervision.

Compliance with ethical standards:

Funding: This project was conducted as part of internal resources from the Indian Institute of Technology Delhi. JKH acknowledges the Institute Scholarship from IIT Delhi for his Ph.D. research, and Miss Sripada acknowledges the award of BTech SURA project by IIT Delhi to work on this project.

Conflict of Interest: Authors declare that they have no conflict of interest.

REFERENCES

Abdul Khalil, H. P. S., Bhat, A. H. and Ireana Yusra, A. F. (2012) 'Green composites from sustainable cellulose nanofibrils: A review', *Carbohydrate Polymers*, 87(2), pp. 963–979.

Adam Mariod, A. (ed.) (2018) *Gum Arabic*. London, UK: Academic Press.

Arshad, K. A., Hirwani, J. K. and Sinha, S. K. (2020) 'Effects of UHMWPE Filler on the Tribological and Mechanical Properties of Biocompatible Epoxies', *Tribology Transactions*, 63(2), pp. 382–392.

Arukalam, I. O., Ishidi, E. Y., Obasi, H. C., Madu, I. O., Ezeani, O. E., and Owen, M. M. (2020) 'Exploitation of natural gum exudates as green fillers in self-healing corrosion-resistant epoxy coatings', *Journal of Polymer Research*, 27(3), p. 80.

Ashori, A. (2008) 'Wood-plastic composites as promising green-composites for automotive industries!', *Bioresource Technology*, 99(11), pp. 4661–4667.

Barari, B., Omrani, E., Dorri Moghadam, A., Menezes, P. L., Pillai, K. M., and Rohatgi, P. K. (2016) 'Mechanical, physical and tribological characterization of nano-cellulose fibers reinforced bio-epoxy composites: An attempt to fabricate and scale the "Green" composite', *Carbohydrate Polymers*, 147, pp. 282–293.

Basak, S. and Ali, S. W. (2017) 'Leveraging flame retardant efficacy of pomegranate rind extract, a novel biomolecule, on ligno-cellulosic materials', *Polymer Degradation and Stability*, 144, pp. 83–92.

Basta, A. H., Abd El-Sayed, E. S. and El-Saied, H. (2004) 'Lignocellulosic materials in building elements. Part IV - Economical manufacture and improvement of properties of lightweight agro-panels', *International Journal of Polymeric Materials and Polymeric Biomaterials*, 53(8), pp. 709–723.

Briscoe, B. J., Evans, P. D., Biswas, S. K., and Sinha, S. K. (1996) 'The hardnesses of poly(methylmethacrylate)', *Tribology International*, 29(2), pp. 93–104.

Briscoe, B. J. and Sinha, S. K. (2003) 'Scratch Resistance and Localised Damage Characteristics of Polymer Surfaces– a Review', *Materialwissenschaft und Werkstofftechnik*, 34(1011), pp. 989–1002.

Chudzikowski, R. J. (1971) 'Guar gum and its applications, *Journal of the Society of Cosmetic Chemists*, 22, pp. 43–60.

Daoub, R. M. A., Elmubarak, A. H., Misran, M., Hassan, E. A., and Osman, M. E. (2018). 'Characterization and functional properties of some natural Acacia gums', *Journal of the Saudi Society of Agricultural Sciences*, 17(3), pp. 241–249.

Das, S. (2017) 'Mechanical properties of waste paper/jute fabric reinforced polyester resin matrix hybrid composites', *Carbohydrate Polymers*, 172, pp. 60–67.

Dickinson, E., Murray, B. S., Stainsby, G., and Anderson, D. M. W. (1988). 'Surface activity and emulsifying behaviour of some Acacia gums', *Topics in Catalysis*, 2(6), pp. 477–490.

Dickinson, E., Elverson, D. J. and Murray, B. S. (1989) 'On the film-forming and emulsion-stabilizing properties of gum arabic: dilution and flocculation aspects', *Topics in Catalysis*, 3(2), pp. 101–114.

Ferreira, S. R. dos S., Mesquita, M. V. N., Sá, L. L. F. de, Nogueira, N. C., Rizzo, M. dos S., Silva-Filho, E. C., Costa, M. P. da, and Ribeiro, A. B. (2019) 'Sustainable natural gums for industrial application: Physiochemical and texturometric evaluation', *Journal of Drug Delivery Science and Technology*, 54(October), p. 101306.

Flores, A., Baltá Calleja, F. J., Attenburrow, G. E., and Bassett, D. C. (2000) 'Microhardness studies of chain-extended PE: III. correlation with yield stress and elastic modulus', *Polymer*, 41(14), pp. 5431–5435.

Grein, A., Da Silva, B. C., Wendel, C. F., Tischer, C. A., Sierakowski, M. R., Moura, A. B. D., Iacomini, M., Gorin, P. A. J., Simas-Tosin, F. F., and Riegel-Vidotti, I. C. (2013) 'Structural characterization and emulsifying properties of polysaccharides of Acacia mearnsii de Wild gum', *Carbohydrate Polymers*, 92(1), pp. 312–320.

Hirwani, J. K. and Sinha, S. K. (2021) 'Mechanical and tribological studies of SU-8 composites filled with UHMWPE and gum acacia under dry and bovine serum albumin lubricated conditions', *Journal of Tribology*, 143(1), pp. 1–15.

Huang, J. K. and Young, W. Bin (2019) 'The mechanical, hygral, and interfacial strength of continuous bamboo fiber reinforced epoxy composites', *Composites Part B: Engineering*, 166(December 2018), pp. 272–283.

Ibrahim, M. M., Dufresne, A., El-Zawawy, W. K., and Agblevor, F. A. (2010) 'Banana fibers and microfibrils as lignocellulosic reinforcements in polymer composites', *Carbohydrate Polymers*, 81(4), pp. 811–819.

Jiang, H., Browning, R. and Sue, H. J. (2009) 'Understanding of scratch-induced damage mechanisms in polymers', *Polymer*, 50(16), pp. 4056–4065.

Khan, Z., Yousif, B. F. and Islam, M. (2017) 'Fracture behaviour of bamboo fiber reinforced epoxy composites', *Composites Part B: Engineering*, 116, pp. 186–199.

Lawn, B. R., Wiederhorn, S. M. and Roberts, D. E. (1984) 'Effect of sliding friction forces on the strength of brittle materials', *Journal of Materials Science*, 19(8), pp. 2561–2569.

Li, M., Pu, Y., Thomas, V. M., Yoo, C. G., Ozcan, S., Deng, Y., Nelson, K., and Ragauskas, A. J. (2020) 'Recent advancements of plant-based natural fiber–reinforced composites and their applications', *Composites Part B: Engineering*, 200, 108254.

Low, I. M., McGrath, M., Lawrence, D., Schmidt, P., Lane, J., Latella, B. A., and Sim, K. S. (2007) 'Mechanical and fracture properties of cellulose-fibre-reinforced epoxy laminates', *Composites Part A: Applied Science and Manufacturing*, 38(3), pp. 963–974.

Maqbool, M., Ali, A., Ramachandran, S., Smith, D. R., and Alderson, P. G. (2010) 'Control of postharvest anthracnose of banana using a new edible composite coating', *Crop Protection*, 29(10), pp. 1136–1141.

Megahed, M., Fathy, A., Morsy, D., and Shehata, F. (2021) 'Mechanical Performance of glass/epoxy composites enhanced by micro- and nanosized aluminum particles', *Journal of Industrial Textiles*, 51(1), 68-92

Monteiro, S. N., Lopes, F. P. D., Barbosa, A. P., Bevitori, A. B., Amaral Da Silva, I. L., and Da Costa, L. L. (2011) 'Natural lignocellulosic fibers as engineering materials-An overview', *Metallurgical and Materials Transactions A: Physical Metallurgy and Materials Science*, 42(10), pp. 2963–2974.

Nirmal, U., Hashim, J. and Low, K. O. (2012) 'Adhesive wear and frictional performance of bamboo fibres reinforced epoxy composite', *Tribology International*, 47, pp. 122–133.

Onuaguluchi, O. and Banthia, N. (2016) 'Plant-based natural fibre reinforced cement composites: A review', *Cement and Concrete Composites*, 68, pp. 96–108.

Padmanabhan, V. P., Kulandaivelu, R. and Nellaiappan, S. N. T. S. (2018) 'New core-shell hydroxyapatite/gum-Acacia nanocomposites for drug delivery and tissue engineering applications', *Materials Science and Engineering C*, 92(July), pp. 685–693.

Radford, K. C. (1971) 'The mechanical properties of an epoxy resin with a second phase dispersion', *Journal of Materials Science*, 6(10), pp. 1286–1291.

Reddy, N. and Yang, Y. (2005) 'Biofibers from agricultural byproducts for industrial applications', *Trends in Biotechnology*, 23(1), pp. 22–27.

Saravanan, P., Satyanarayana, N. and Sinha, S. K. (2013) 'Self-lubricating SU-8 nanocomposites for microelectromechanical systems applications', *Tribology Letters*, 49(1), pp. 169–178.

Sarkar, P., Modak, N. and Sahoo, P. (2018) 'Mechanical and Tribological Characteristics of Aluminium Powder filled Glass Epoxy Composites', *Materials Today: Proceedings*, 5(2), pp. 5496–5505.

Satyanarayana, K. G., Arizaga, G. G. C. and Wypych, F. (2009) 'Biodegradable composites based on lignocellulosic fibers-An overview', *Progress in Polymer Science (Oxford)*, 34(9), pp. 982–1021.

Satyanarayana, K. G., Guimarães, J. L. and Wypych, F. (2007) 'Studies on lignocellulosic fibers of Brazil. Part I: Source, production, morphology, properties and applications', *Composites Part A: Applied Science and Manufacturing*, 38(7), pp. 1694–1709.

Singh, B., Sharma, S. and Dhiman, A. (2017) 'Acacia gum polysaccharide based hydrogel wound dressings: Synthesis, characterization, drug delivery and biomedical properties', *Carbohydrate Polymers*, 165, pp. 294–303.

Sinha, S. K., Song, T., Wan X., and Tong, Y. (2009) 'Scratch and normal hardness characteristics of polyamide 6/nano-clay composite', *Wear*, 266(7–8), pp. 814–821.

Spanoudakis, J. and Young, R. J. (1984) 'Crack propagation in a glass particle-filled epoxy resin', *Journal of Materials Science*, 19(2), pp. 487–496.

Tabor D (1970) 'The hardness of solids', *Rev Phys Technol*, 1(3), pp. 145–179.

Verbeken, D., Dierckx, S. and Dewettinck, K. (2003) 'Exudate gums: Occurrence, production, and applications', *Applied Microbiology and Biotechnology*, 63(1), pp. 10–21.

Wan, Y. J., Gong, L. X., Tang, L. C., Wu, L. Bin, and Jiang, J. X. (2014) 'Mechanical properties of epoxy composites filled with silane-functionalized graphene oxide', *Composites Part A: Applied Science and Manufacturing*, 64, pp. 79–89.

Whistler, R. L. and BeMiller, J. N. (2012) *Industrial Gums: Polysaccharides and Their Derivatives: Third Edition*, *Industrial Gums: Polysaccharides and Their Derivatives: Third Edition*.

Williams, P. A. and Phillips, G. O. (2009) 'Gum arabic', *Handbook of Hydrocolloids: Second Edition*, pp. 252–273.

Yang, J., Ching, Y. C. and Chuah, C. H. (2019) 'Applications of lignocellulosic fibers and lignin in bioplastics: A review', *Polymers*, 11(5), pp. 1–26.

Youssef, A. M., Hasanin, M. S., Abd El-Aziz, M. E., and Darwesh, O. M. (2019) 'Green, economic, and partially biodegradable wood plastic composites via enzymatic surface modification of lignocellulosic fibers', *Heliyon*, 5(3), p. e01332.

Zhang, Z., Cai, S., Li, Y., Wang, Z., Long, Y., Yu, T., and Shen, Y. (2020) 'High performances of plant fiber reinforced composites—A new insight from hierarchical microstructures', *Composites Science and Technology*, 194(February), p. 108151.

